AD

TECHNICAL REPORT

72-24-FL

MICROWAVE APPLICATIONS TO FREEZE DEHYDRATION. PRELIMINARY EVALUATION OF A 2450 MHz SYSTEM.

by

J. W. Gould

J. T. Perry, Jr.

E. M. Kenyon

February 1972

UNITED STATES ARMY
NATICK LABORATORIES
Natick, Massachusetts 01760

Food Laboratory

FL-146

This document has been approved for public release and sale; its distribution is unlimited.

Citation of trade names in this report does not constitute an official indorsement or approval of the use of such items.

Destroy this report when no longer needed. Do not return to the originator.

This document has been approved for public release and sale; its distribution is unlimited.

AD_____

TECHNICAL REPORT

72-24-FL

MICROWAVE APPLICATIONS TO FREEZE DEHYDRATION – PRELIMINARY EVALUATION OF A 2450 MHz SYSTEM

by

James W. Gould
John T. Perry, Jr.
Ernest M. Kenyon

Project reference:
1-J662713A034

February 1972

Series: FL-146

Food Laboratory
US Army Natick Laboratories
Natick, Massachusetts 01760

FOREWORD

The use of microwave heating has long been suggested as a means of accelerating the freeze drying process. Microwave heating bypasses the heat transfer limitations of conventional freeze drying and rates 3 to 10 times as fast are possible. Prior literature of the process, however, has been either empirical or theoretical, with little correlation of the two into a unified model.

This paper derives a generalized theory of microwave freeze drying and compares it to the authors' experimental data on freeze drying of raw steak at 2450 MHz. At operating pressures of about 1.0 Torr, cycle times of 185 minutes for 3/8 inch thick steak were obtained. The frequency variation of corona breakdown field strength is discussed and applied to freeze dehydration. The effect of cavity wall losses, quantity, thickness, dielectric properties of the food itself, and gas pressure and composition in the vacuum chamber are related to rates of freeze drying.

A corrected form of the power equation using a power absorption factor instead of the simple loss factor is indicated for determining dielectric power absorption in a resonant cavity. The corrected form is used to predict drying rates which compare favorably to experimental data.

TABLE OF CONTENTS

	Page No.
Abstract	iv
List of Figures	v
List of Symbols	vi
Introduction	1
Theory of Corona Breakdown and Power Absorption	1
Theory of Mass Transfer	4
Experimental Apparatus and Method	4
Data and Discussion	5
Conclusion	11
References	12
Appendix I	13
Appendix II	15

ABSTRACT

A generalized model of microwave freeze dehydration is presented including the efficiency of power absorption, the mass flow rates of water and water vapor, and the parameters characterizing corona breakdown at the 2450 MHz operating frequency. The effect of chamber pressure, gas composition, size and thickness of the food load, and the operating frequency are discussed theoretically and compared to experimental data for freeze dehydration at 2450 MHz. The agreement between the theoretical and experimental mass flow rates was good for the majority of the dehydration cycle.

LIST OF FIGURES

Figure Number

1. Breakdown fields vs pressure for air, water, and CO_2 at 2450 MHz $\Lambda = 0.67$
2. Experimental and theoretical breakdown fields for air at 915 MHz and 2450 MHz
3. Block diagram of experimental microwave freeze drier
4. View of control console, bidirectional coupler, dummy loads, waveguide switch and water load
5. View of vacuum chamber and condenser
6. Front view of cavity showing food tray, scale, and rotator
7. Freeze dried steaks from determination of maximum drying rate; runs XI, XII, XIII and XX violated triple point; runs XXIII and XXIV did not
8. $\beta\epsilon_c''$ and loss factor, ϵ_r'', vs temperature for raw steak
9. $\beta\epsilon_c''$ and loss factor, ϵ_r'', va temperature for H_{20}
10. Weight of food and power absorbed by the food vs time for a typical freeze dry cycle with two 1/4-inch steaks
11. Efficiency of power absorption vs weight. $K = 0.39 \times 10^{-3}$
12. Measured flow rate, M_a and theoretical flow rate, M_e vs time for a typical freeze drying cycle of two 1/4-inch thick steaks
13. Interface pressures calculated on energy balance basis and a mass flow rate basis vs time for a typical freeze drying cycle. Measured chamber pressure is also shown.
14. Electric field, breakdown field, and power input vs time for a typical freeze drying cycle for two 1/4-inch thick steaks.

LIST OF SYMBOLS

Symbol	Description
E_o	Free space electric field, volts/cm
K	Wall loss constant
A	Area of surface of frozen food
G	Permeability constant
Q	Rate of ice sublimation, grams/hour
M_e	Mass flow rate from weight loss
P_i	Interface pressure
P_B	Chamber pressure
T_P	Peak to peak pulse time
t_p	Non-zero portion of the power pulse
V	Cavity volume
X	Thickness of the dried layer
φ	Efficiency of power absorption
ϵ_r''	Loss factor
ϵ_r'	Dielectric constant
ϵ_c''	Power absorption factor
Λ	Diffusion length-cm.

INTRODUCTION

The use of microwaves to accelerate the freeze drying of food is not a new concept. It has been suggested and investigated by several people (1,2,3,4). Microwaves bypass the heat transfer limitations of conductive or radiant heating by preferential heating of the frozen portion of the food; thus the process becomes mass transfer limited rather than heat transfer limited. While experimental work supports the contention that a faster process is possible, the question of overall economics is still unresolved. An analysis by Grimm (5), for example, used the conclusion of Hoover *et al* (1,2) that very low (50 to 60 microns) pressures are needed to avoid corona breakdown. Parker (6) and Gould (7), however, indicate a strong frequency dependence of corona breakdown and suggest that the economic analysis of Grimm at 915 MHz may not hold for other frequencies such as 2450 MHz.

The purpose of this paper is not, however, a detailed economic analysis of microwave freeze drying. Rather it reports cycle times and typical operating parameters for microwave freeze drying of slow frozen raw beef at 2450 MHz. The breakdown theory of Gould (7) was also tested for typical freeze drying cycles. An expression for the theoretical efficiency of power absoprtion by the food throughout the cycle was derived and tested against experiment. Lastly, a crude check of mass transfer rates across the dried layer was calculated from the permeability data of Bralsford (8).

The theory involved in the various tests was sufficient to have meaning for scale-up, and the qualitative economics of changing frequency were inferred from the results of theory and experiment.

THEORY OF CORONA BREAKDOWN AND POWER ABSORPTION

Corona breakdown is important in freeze dehydration studies because the breakdown field is an upper limit to the amount of power that can enter the microwave cavity. The ionization of gas molecules, which produces a plasma or corona, can scorch the food and thus cause detrimental effects to the freeze dehydration process.

The electric field necessary for breakdown is a function of gas pressure, temperature, and composition, cavity size, and the propagation frequency. For freeze drying, the gas consists of air and water vapor with varying total and partial pressures throughout the cycle. Figure 1 shows breakdown curves for air, water vapor, and CO_2 at 2450 MHz for the cavity used by the authors. Note that the minimums of the curves are at different pressures, and that the curves for air and water vapor intersect at 2 Torr. Thus, depending on the total pressure, increasing the partial pressure of air by bleed-in may increase or decrease the breakdown field. The CO_2 curve was included as a possible bleed-in gas, however it unfortunately turned out to be worse than air.

The exact effect of cavity size and geometry is beyond the scope of this paper, but in general, a larger cavity will give lower breakdown fields. The effect diminishes after a point though so that increasing the cavity dimensions beyond a few centimeters has little effect; hence, the variation of breakdown fields with cavity size has little importance for industrial size freeze driers.

Pressure has a strong effect on breakdown fields, as shown in Figure 1. Temperature variation is calculated by reducing all pressures to a standard temperature of 25°C. Why breakdown is a problem in freeze drying can be seen from the pressure region of the minima of the curves: the pressures are the same as freeze drier operating pressures. Hoover *et al* (1), avoided breakdown during their studies by reducing the pressure.

A change in pressure from 1.0 Torr to 0.1 Torr (see Figure 2), at 915 MHz increases the breakdown field from 84 volts/cm to 210 volts/cm (for size cavity used by the authors). Since the power absorbed by the food is proportional to the square of the electric field, the power can be increased by a factor of 6.25.

Another way breakdwon may be avoided is to change the frequency. If the pressure is held at 1.0 Torr and the frequency changed from 915 to 2450 MHz, the limiting field will be increased from 85 volts/cm (915 MHz theory) to 230 volts/cm (2450 MHz experimental). It thus appears that good rates are possible at 2450 MHz at 1.0 Torr. The problem arises in relating the field to the input power. Coupling loops, bolometers, and other instruments in the cavity disturb the field itself and/or require equipment which would not be easily used by untrained personnel on an industrial scale. RF power, on the other hand, is easily and cheaply measured, and can be related to electric field as follows:

With a forward reflected power meter or a bi-directional coupler, measure the power in the Power Reflected from the cavity. Then follow the following steps to determine the electric field strength:

1. Determine the power absorbed by equation (1)

   Power Absorbed = Power In - Power Reflected (1)

2. Assuming negligible losses between the meter and cavity the power can only be absorbed by wall losses in the cavity or by the dielectric load. Thus the Power Absorbed is divided into two parts as explained by equation (2).

   Power Absorbed = wall loss + dielectric loss (2)

3. The wall loss can be expressed as:

$$\text{Wall loss} = KE_0^2 \qquad (3)$$

The constant K is the wall loss constant which is analogous to the admittance of a lumped circuit. See Appendix I for the determination of K for an arbitrary cavity.

4. The remaining power is absorbed by the dielectric load according to equation (4) as follows:

$$\text{Dielectric Loss} = \frac{8.84 \times 10^{-14}\ 2\pi f\ \epsilon_r''\ E^2 V}{(\epsilon_r')^2 + (\epsilon_r'')^2} \qquad (4)$$

Equation (4) is the familiar power equation correct for the reduction of the free space field inside the dielectric.

5. In the case of a pulsed output the dielectric loss equation is multiplied by the ratio t_p/T_p which is the ration of the non-zero power portion of the pulse to the peak to peak pulse time.

6. For n dielectric loads (food, racks, trays) the electric field is then:

$$E = \frac{\text{Power in} - \text{Power Reflected}}{K + C_1 + C_2 + \ldots + C_n} \qquad (5)$$

The maximum theoretical power absorbed without breakdown was calculated from the E_o given by Figure1 for the measured pressure by substituting into a rearranged equation (5).

$$\text{Power Absorbed} = E_o\ (K + C_1 + C_2 + \ldots + C_n) \qquad (6)$$

The power given by equation (6) was then compared with experimental breakdown power. The fraction of power absorbed by the food load C_1 was derived from equation (6) without knowing the electric field.

Equation (7) shows how this can be done.

$$\varphi = \frac{\text{Power absorbed by food}}{\text{Total Power Absorbed}} = \frac{E_0^2\ C_1}{E_0^2\ (K + C_1 + C_2 + \ldots C_n} \qquad (7)$$

A calculation of the watts absorbed by the food from equation (4) can be converted to grams of ice sublimed per hours by dividing by 0.783. This theoretical sublimation rate was called M_e (mass flow rate based on energy balance) and was compared to the follow rate determined from the actual measured weight loss, M_a.

THEORY OF MASS TRANSFER

Detailed analysis of the mechanisms of the mass flow of water vapor through the dried food layer requires a knowledge of pore size, capillary tortuosity, gas viscosity, and the average temperature of the dried layer (13). To simplify the analysis, the macro approach of Bralsford (8) was used.

$$Q = \frac{G\ A\ (P_i - P_B)}{X} \qquad (8)$$

For raw, slow frozen freeze dried beef, Bralsford gives a value for G of (4.4 ± 1.5) x 10^{-5} gm sec^{-1} cm^{-1} $Torr^{-1}$, or approximately 0.016 gr hr^{-1} cm^{-1} $Torr^{-1}$. Knowing the interface pressure, equation (8) can be used to get Q, or setting Q equal to M_a, the interface pressure can be back calculated from the following equation:

$$P_i = \frac{M_a\ X + P_B}{G\ A} \qquad (9)$$

Care must be taken to use the area corresponding to the experimental conditions. For the present experiments, the area used was the total of the top and the bottom areas since the tray supporting the food was performated.

EXPERIMENTAL APPARATUS AND METHOD

The experimental equipment used for these studies is shown in block diagram form in Figure 3. Pictures of the equipment are shown as Figures 4, 5, and 6. The bi-directional coupler-oscilloscope assembly shown in Figure 3 can be replaced with a forward-reverse reading power meter. Further discussion of the equipment is given in Appendix II.

Since there was no way to directly measure the interface pressure of temperature, the maximum mass flow rate from equation (8) could not be determined and converted to an optimum power input via equation (8). Instead, the maximum power was found empirically by starting at power levels high enough to violate the triple point, then reducing the power by increments until a good product was obtained. Figure 7 shows typical results of these runs. In Figure 7:

Run XI:	High power with no rotation
Run XII:	Low power with no rotation
Run XIII:	Medium power with rotation
Run XX:	High power with rotation
Run XXIII:	Low power with rotation

After the optium power levels were found for each load of steak, sufficient samples were run to establish typical curves of total weight, mass flow rate, power in and power reflected, total pressure, partial pressure of water vapor, and breakdown power throughout the drying cycle. Because of the power limitations of the RG 14 A/U cable transition into the vacuum chamber, the breakdown power could only be determined for the end of the cycle using equation (5). This value was then compared with the theoretical breakdown value and empty cavity breakdown fields show in Figure 2.

DATA AND DISCUSSION

To simplify predicting the effect of the changing dielectric load, C, of the food, the power absorption factor was defined as:

$$\epsilon_c'' = \frac{\epsilon_r''}{(\epsilon_r')^2 + (\epsilon_r'')^2} \tag{10}$$

and a constant β such that:

$$\beta = 2\pi f \; 8.84 \times 10^{-14} \; (t_p/T_p) \tag{11}$$

which at 2450 MHz and a value of 0.743 for (t_p/T_p) reduced to:

$$\beta = 1.0 \times 10^{-3} \tag{12}$$

From the data of Kan (14), the values of $\beta\epsilon_c''$ (called CPVOL in the Figure) were plotted for various temperatures as in Figure 3. The unexpected result of the plot was a peak at -13.4°C, even though the loss factor ϵ_r'' continually decreased as temperature increased.

Although this seems to contradict the Power Equation and the accepted concept of preferential heating of thawed food over frozen food, the form of ϵ_c' is the more correct one for expressing dielectric loads. If the loss factor is used rather than the power absorption factor a dielectric loading is given which is too large by a factor of two (see Figure 8).

The apparent contradiction lies in the implicit assumption in the Power Equation that the E^2 term refers to the field inside the dielectric. Wall loss, however, is determined by the free space field in the cavity. Therefore, one or the other E must be converted so that both losses are based on the same E. If we wished, the field inside the dielectric, E_d, could be the common term, but the value of K would then be increased by a factor of $((\epsilon_r')^2 + (\epsilon_r'')^2)$ and the net effect on equation (7) would be the same. E_o is used here because it determines gas breakdown.

The $\beta\epsilon_c''$ value times the volume of the frozen food, V, gives the dielectric load of the food, C_1. Knowing K, substitution in equation (7) gives the efficiency of power absorption, φ. Multiplying (Power in - Power Reflected) by φ gives the watts absorbed by the food. Figure 10 shows the calculated absorbed power of the food over a typical cycle for two 1/4-inch steaks with total weight of 69 grams. The input power is also noted for the cycle. It is instructive to recall that the slope of the weight-time curve should be proportional to the power absorbed by food. In other words, the maximum mass flow should occur at maximum absorbed power, which is shown at about 50 minutes on Figure 10. The two 1/4-inch steaks were used instead of a single 1/2-inch steak because the authors did find a difference in rates with varying thickness, contrary to the conclusions of Hoover (2). Guido, *et al.* (16) suggested that Hoover did not use sufficient input power and therefore did not operate at the limits of maximum mass transfer. This is only partially correct because we are really concerned with absorbed power rather than input power.

Hoover (2) pro-rated the power input on a weight basis (double the weight, double the power). However, the maximum drying rates on an energy basis are proportional to efficiency. Figure 11 shows calculated efficiencies for initial loads of 100, 50, and 24 grams of steak at -15°C. The 100 and 50-gram loads are comparable to a 1/2-inch and 1/4-inch steak. When a 100-gram steak is half dry, the efficiency has changed from 89 to 81%, while for the 50-gram steak, the efficiency drops from 81 to 68%. For 75% dryness, the 100-gram steak has 65% efficiency, and the 50-gram steak has 51%.

The $\beta\epsilon_c''$ peak is sharp for phase changes of pure substances. Figure 9 shows $\beta\epsilon_c''$ and ϵ_r'' vs temperature for pure water at 3000 MHz, using the dielectric constant and loss factor values of Von Hippel (15). The work of investigators who obtained very low sublimation rates for pure ice would fall far below 0°C. giving a lower power absorption factor. Qualitative checks by the authors showed better coupling to ice at -0°C. than an equivalent volume of water at 25°C, which could support either curve of Figure 9. A qualitative check with steak, however, supported the power absorption factor form of Figure 8. The final proof will lie in the ability to predict theoretical rates.

The steak power absorption factor does not drop off as fast as ice at temperatures below the peak because of the amorphous state of frozen beef. The shape of the power absorption factor curve supports the theory of bound water not being frozen out at some finite temperature, but rather a gradual process of increasing concentration of a non-frozen solution.

Thus, doubling the weight and power input while going from 1/4-inch to 1/2-inch steaks will give mass flow rates more than twice as fast. This explains the data of Hoover in Table 1 a, which gives drying times for varying thicknesses of hamburger patties.

Table 1 a

Drying Rates of Hamburger Patties

(915 MHz, 0.06 Torr chamber pressure, 15-60 watts)

Thickness (inch)	Number of Samples	Drying Time (minutes)
0.25	1	142
0.50	1	130
0.75	1	138
1.00	1	145

Thicknesses greater than 0.50 inch probably cause mass transfer limitations, and the rate decreases again.

Table 1 b shows the drying rates for raw steak at 2450 MHz. The table shows the decrease in drying times for doubling the load at the same thickness and the increase of the drying time for increasing the thickness. The mass transfer limit was reached at thinner samples by the authors because of the higher chamber pressure used.

Table 1 b

(2450 MHz, 1.5 Torr chamber pressure, 10-45 watts)

Thickness (inch)	Number of Samples	Drying Time (minutes)
0.25	1	185
0.25	2	180
0.375	1	210
0.375	2	197

Even if the power is not pro-rated by weight, the efficiency curves of Figure 11 still operate to give an upper limit to drying rates. This is because the maximum E_o is determined by the breakdown limitation and is independent of loading. Notice that the breakdown field is given by Figures 1 and 2. Equation 6 merely relates the field for a given cavity to the load and power level. Therefore, the maximum power that can be absorbed by the food is simply C times the square of the breakdown field strength.

Also included in Figure 11 is a curve showing the effect of a larger skin loss constant, K. The larger K causes lower efficiencies throughout the drying cycle and lower maximum mass flow rates. Fortunately, the inverse of the cavity Q_u, $1/Q_u$, (and therefore K-- See Appendix 1) is roughly proportional to the cavity area to volume ration, which for a cube of side X is 6/8. Thus the scale up to larger cavities and larger loads of food should decrease K, increase C, and hence increase the efficiency of power absorption, φ.

Nevertheless, a detailed economic analysis should use the decrease in efficiency throughout the cycle when calculating the microwave energy cost. Grim (5) used this type of detailed analysis in his economic survey using the data of Hoover (1, 2).

As stated above, the final proof of the effectiveness of the power loss factor is a comparison of actual flow rates and theoretical flow rates. Figure 12 shows the results of M_a and M_e over a typical cycle. The lower M_a for the first 40 minutes is probably due to the microwave energy heating the food to a temperature at which the vapor could sublime, rather than sublimation of the ice. Between two and six grams of ice were sublimed during the 10-minute pumpdown, and the heat of sublimation came mostly from cooling of the food. As the food warmed up and the interface pressure increased, the M_a increased to equal and exceed the M_e. This could be due to the peculiar temperature profiles of homogeneous internal heat generation. For this case, the center temperature is higher than the interface temperature. At about 40 minutes elapsed time (see Figure 12), the conductive heating of the interface from the center of the food caused a sharp rise in flow rate; but, the increased flow rate removed more of the heat of sublimation, and after a short time a dynamic equilibrium was established and M_a equaled M_e for the remainder of the run.

The points for the theoretical M_e curve were calculated by a computer program. Also plotted on Figure 12 are the computer selected temperatures for determination of the power absorption factor. The deviations from a smooth curve are caused largely by the large standard deviation of the regression analysis used in the program to calculate the power absorption factor as a function of temperature. Also, the first three points were caused by the program not being sophisticated enough to allow for internal heating or cooling of the food. The dashed line is probably closer to the true average temperature of the frozen layer. The dried food temperature is expected to rise near the end of the cycle as its loading approximates the loading of the small amount of frozen food left. Again, the simplified computer program did not allow for this effect and showed temperatures dropping throughout the end part of the cycle.

The program also calculated two interface pressures, one from the equilibrium ice vapor pressure for the calculated power loss factor and the other from the mass flow pressure drop as expressed in equation (1). Figure 13 shows the two calculated interface pressures over a typical freeze dry cycle along with the measured chamber pressure. The difference between the chamber pressure and the interface pressure is a measure of the pressure drop across the dried layer of food. Although this pressure drop increased as the dried layer thickness increased, it decreased with the falling mass flow rate through the later part of the cycle. The two effects oppose each other to give a fairly uniform pressure drop of 0.10 to 0.20 Torr.

The variation of the energy basis calculation of the pressures at the interface in the beginning and end of the cycle are due to the inaccuracies of the program as described above. The correlation of the two pressures is a measure of the agreement between the energy balance and mass transfer analysis of the process. While agreement is good for the middle range (Region II) of the cycle, the beginning and end (Regions I and III) require more detailed analysis.

Lastly, the program calculated the electric field throughout the cycle, as shown in Figure 14. The input power and breakdown field for the measured chamber pressure from Figure 1 are also plotted. The breakdown field remained essentially constant at 200 volts/cm throughout most of the cycle even though the chamber pressure varied. This was due to the changing gas composition. Reference to Figure 1 again showed that a decrease from two Torr total pressure (mostly air) to one Torr total pressure (half air and half water vapor) does not change the breakdown field. Near the end of the cycle, the breakdown field increases as the partial pressure of water and the total pressure decrease and the higher breakdown strength of air predominates.

Theory predicts that corona breakdown is not limiting for the run shown, and the experiment verified this. Table 2 shows a comparison of theoretical and measured power for breakdown for various loads near the end of the cycle.

Table 2

Theoretical and Experimental Breakdown Power

Loads	Theoretical Absorbed Power (watts)	Experimental Absorbed Power (watts)
0.832×10^{-3}	48.8	43.5
0.88×10^{-3}	50.8	50.8
0.67×10^{-3}	36.3	35.4
0.195×10^{-3}	42.6	41.2

Experience showed that mass transfer limitations were more stringent than breakdown limitations except in the case of light dielectric loading. Changing from 915 MHz to 2450 MHz has the effect of shifting the process from breakdown limited to mass flow limited while allowing average operating pressures of 1.5 Torr.

These data indicate that the economic analysis of Grimm (5) may hold for 915 MHz but not for 2450 MHz. For the higher frequency, the analysis of Decareau (17) is more applicable. Assuming 5 kW magnetrons with 50% efficiency, the calculated microwave freeze drying costs are 5.24 cents/lb of water removed as compared with 5.02 cents/lb for radiant freeze drying. In the eight years since the study, the cost /kilowatt has changed and the efficiences have increased. Another detailed analysis is needed to update the exact economics, but the authors feel the comparison will be favorable.

Lastly, a preference test and a triangle test were run to compare radiant and microwave freeze dried steak. The preference test showed no significant difference, while the triangle test showed significance at the 5% confidence level. While larger samples are needed to resolve the question, the differences cited by the taste panel in the triangle test were not consistent enough to say that the microwave steaks were different in flavor, tenderness, etc. Other researchers in microwave freeze drying have found the microwave processed foods acceptable.

CONCLUSIONS

Raw steaks have been routinely dried in three hours at average operating pressures of 1.5 Torr and microwave power at 2450 MHz. The drying was done in a multimode cavity with rotation of the sample to reduce the effect of hot spots. Theory was derived to determine drying rates, efficiences of power absorption, breakdown fields, and interface pressures. This theory is supported by experimental data. The efficiency of the process is predicted by the theory to increase during scale up due to the larger dielectric load.

The use of ϵ_c'' instead of ϵ_r'' in the authors' corrected power equation indicates a peak absorption for raw steak at -13.4°C, even though ϵ_r'' decreased throughout that temperature region. Thus, while melting can occur from too much power absorption by violating the triple point, the concept of a "runaway" (heating of the thawed portion of the expense of freeze drying is not applicable, since (at least for raw steak) the power couples better at -13.4°C than at 0°C. This corrected form is applicable in general to heating in resonant cavities when the skin loss is known and the load occupies enough volume to even out the hot and cold spots of field intensity.

The economics of microwave freeze drying appear more favorable at 2450 MHz largely because of the higher breakdown fields associated with the higher frequency. Using the authors' theory, it should be possible to optimize the process. While radiant freeze drying optimization tries to maximize mass permeabilities and power absorption efficiencies. Not all foods should be expected to yeild fast rates because of the relative permeabilities. The past history of the food is also important (e.g. the permeability of slow frozen steak (large crystals) is over three times as large as that of quick-frozen (small crystals) steak (8)). Also, the salting of meat or sugaring of fruits may help or hinder microwave freeze dehydration by changing the power absorption factor dependence on temperature (16).

The present paper has far from exhausted the field. Rather, the authors have tried to prove the effectiveness of microwave freeze drying in multimode cavities at normal freeze drying pressures through theory and experiment. Much more experimentation is needed on product types and treatment, and the problems of scale up. The theory given here, however, should simplify the work by allowing comparison between various cavity designs, operating parameters and foods on a theoretical base rather than a strictly empirical one. The process is too complex to depend on trial and error for each individual freeze drier and each individual food. It is hoped that future work will refine the theory to allow for temperature transients, the differing mechanisms of mass transfer throughout the cycle, and heating of the dried food layer with a goal of optimizing industrial scale microwave freeze driers and products.

REFERENCES

1. Hoover, N.W., Markanonatos, A. Parker, W.N.; "Experimental Accelerated Freeze-drying of Foods by Means of UHF Dielectric Heating"; Food Technology 20: 807-14 June 1966.

2. Hoover, *et al*, "Engineering Aspects of Using UHF Dielectric Heating to Accelerate the Freeze Drying of Foods", Food Technology 20: 807-14 June 1966.

3. Copson, David A., *Microwave Heating,* AVI Publishing Co., Westport, Conn. 1962.

4. Cotson, S., Smith, D.B., *Freeze Drying of Foodstuffs,* Columbia Press, London, 1963.

5. Grimm, A.C., "A Technical and Economic Appraisal of the Use of Microwave Energy in the Freeze-Drying Process", ST-3980, RCA Review, Dec. 1969.

6. Parker, W.N., "Freeze Drying", *Microwave Power Engineering,* Vol. 2, Academic Press, N.Y. 1968.

7. Gould, J.W., Kenyon, E.M., "Corona Breakdown and Electric Field Strength in Microwave Freeze Drying", presented at International Microwave Power Institute Conference (IMPI), Oct. 1970, The Hague, Netherlands.

8. Bralsford, R., "Freeze Drying of Beef", Food Technology, 1967-2 PP339-352.

9. Campbell, Ali Bulent, *Plasma Physics and Magnetoflindmechanics*, McGraw Hill, N.Y., 1963.

10. Francis, G., *Ionization Pheonomena in Gases*, Academic Press, N.Y., 1962.

11. Brown, S.C., *Basic Data of Plasma Physics*, MIT Press, Cambridge, MA, 1966.

12. MacDonald, A.D., *Microwave Breakdown in Gases*, J. Wiley & Sons, N.Y., 1966.

13. Harper, John C., "Transport Properties of Gases in Porous Media at Reduced Pressures with Respect to Freeze Drying", AICHI Journal, July 1962, PP 298-302.

14. Kan, B., "Improving Upon Removal and In-process Moisture Determination", Quartermaster Research Contract #DA-19-129-QM-1546.

15. Van Hippel, A.R., *Dielectric Materials and Applications*, J. Wiley & Sons, N.Y., 1958.

16. Guigo, E.I., Malkov, L.S., Kaoukhtchechuili, E.I., "Center Properties of Heat Mass Transfer During the Freeze Drying of Porous Materials in an UHF Field" in "Symposium on Thermodynamic Aspects of Aspects of Freeze Drying," International Institute of Refrigeration, Commission X, Lausanne, Switzerland, 1969.

APPENDIX I

Determination of K

The value of K may be determined from theory of experiment:

Experiment

The value of K can be determined for a given cavity by measuring Power in and Power out for the empty cavity just before breakdown.

$$K = \frac{(\text{Power in Power out})}{E_0^2} \qquad \text{(A1)}$$

To find the breakdown field, use a pressure above about 10 Torr so that the effect of differing cavity size and shape is eliminated. The electric field at breakdown for dry air is then expressed by:

$$E_e/p = 32 \text{ volts/cm} - \text{Torr} \qquad \text{(A2)}$$

where E_e the effect field is:

$$E_e = \frac{E_{rms}}{1 + \frac{W^2}{V_c^2}^{1/2}} \qquad \text{(A3)}$$

W = field frequency, radians per second

V_c = electron collision frequency for air

$V_c = 5.3 \times 10^9 p$, p in Torr

If $p\,\lambda$ is greater than 100 Torr-cm (λ = wavelength of applied field), then $E_e = E$ and breakdown becomes independent of frequency. For this case, literature values of breakdown fields can be used directly. One determination of K is good for all power levels, but a number of replicates is urged to get a good average because of the randomness caused by the presence or lack of free electrons to initiate the process. The K for the authors' cavity was determined by experiment to be 0.39×10^{-3}.

Theory

An expression for the skin loss constant K can be derived from the cavity Q as:

$$E_o = \sqrt{\frac{P_o Q_u}{\eta w_o}} \qquad \text{(A4)}$$

P_o = power absorbed in empty cavity at resonance

E_o = maximum electric field in cavity

W_o = resonant frequency, radians/sec

$Q_u = 2 \dfrac{\text{Energy stored in cavity per cycle}}{\text{Energy lost in cavity per cycle}}$

$n = \doteq b\epsilon_0 v$

b = constant of electric field distribution such that:

$(E_f \text{ average})^2 = b\ (E_o)^2 = (E_f \text{ breakdown})^2$

E_o = free space permittivity, 8.84×10^{-14} farad/cm

V = volume of cavity, cm^3

Rearranging A4 gives:

$$K = \frac{nw_0}{Q_u} \qquad \text{(A5)}$$

Equation A5 shows K to be independent of electric field and power as stated above.

Harvey (18), gives the theoretical Q_u for various dominant modes in resonant cavities. For the TE 202 mode of the author, Harvey (18) gives:

$$Q_u\delta_s = \frac{ABC}{2} \frac{[(\ell/A)^2 + (n/c)^2]^{3/2}}{(^1/A)^2\ C(A+2B) + (\frac{n}{c})^2 C + 2B} \qquad \text{(A6)}$$

m,n, are eigen values of TE_{mnl}

A, B, C are dimensions of cavity, cm

δ_s is the skin depth of the cavity walls in cm at the resonant frequency.

Substituting appropriate values for the authors' cavity (A=B=C=25.4 cm; $m = \ell = 2, n = 0$; $b = (0.707)^2$ for half sinusoidal distribution) gives a theoretical K of 0.37×10^{-3}, which corresponds well to the empirical value of 0.39×10^{-3}.

APPENDIX II

Microwave Equipment

The microwave energy source is an Amperex DX-260 one kilowatt magnetron with a full wave rectified power supply, giving pulsed output at 120 Hz. A circulator shunted the reflected power to a dummy load to protect the source. The RF power was then directed to an H-tuner to provide control over the power level. Unused power was shunted to a dummy load. The power then pass through a monitoring system in which a bidirectional coupler and crystal detector were used to provide a signal to be monitored on an oscilloscope. The power then passed through a microwave switch and was sent to a water load or to the cavity. The power levels were calibrated by means of a thermophile and millivoltmeter which monitored the temperature rise of the water passing through the water load.

A cubic cavity was used, approximately two wavelengths on each side, and supported a dominant TE 202 mode. The food load in the cavity rested on a perforated polyethylene tray, supported from the scale by nylon monofilament line. The vacuum chamber was a converted autoclave with doors at each end and Plexiglass window through which the scale was viewed. A metal screen over the window blocked RF leakage. The cavity was perforated top and front for removal of water vapor, and a mirror was hung from the top of the vacuum chamber to allow viewing the food while drying.

Total pressure was read by a 0-100 Torr diaphram gauge and an 0-5 Torr gauge. The exhaust line had a hygrometer probe to measure the partial pressure of water vapor independent of the total pressure. The reading on the meter was converted from frost point temperature to the equilibrium vapor pressure of ice. A vapor trap cooled by dry ice and ethanol to -77°C provided the condenser, and a vacuum pump removed noncondensables.

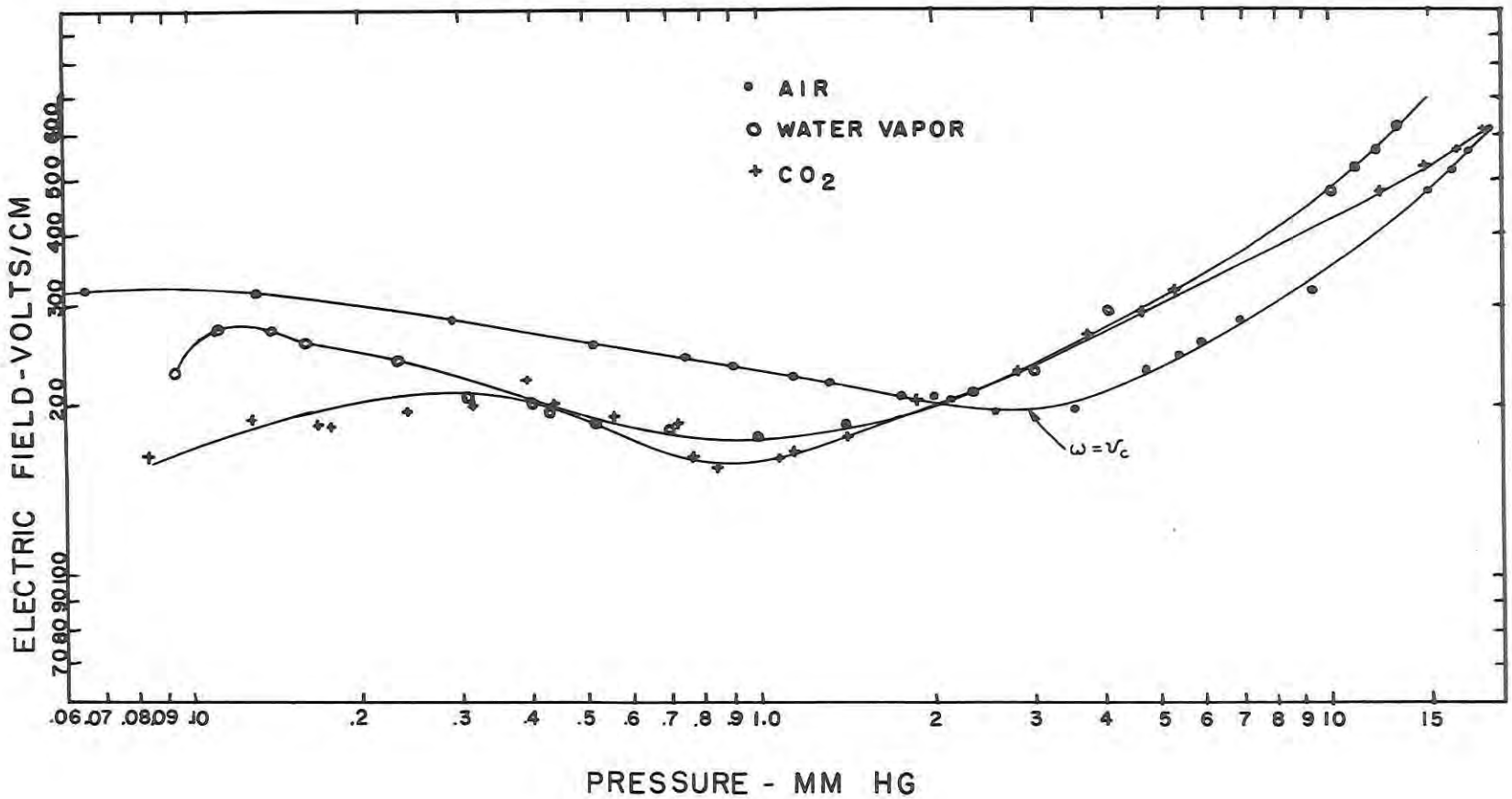

Figure 1. Breakdown fields vs pressure for air, water, and CO_2 at 2450 MHz $\Lambda = 0.67$

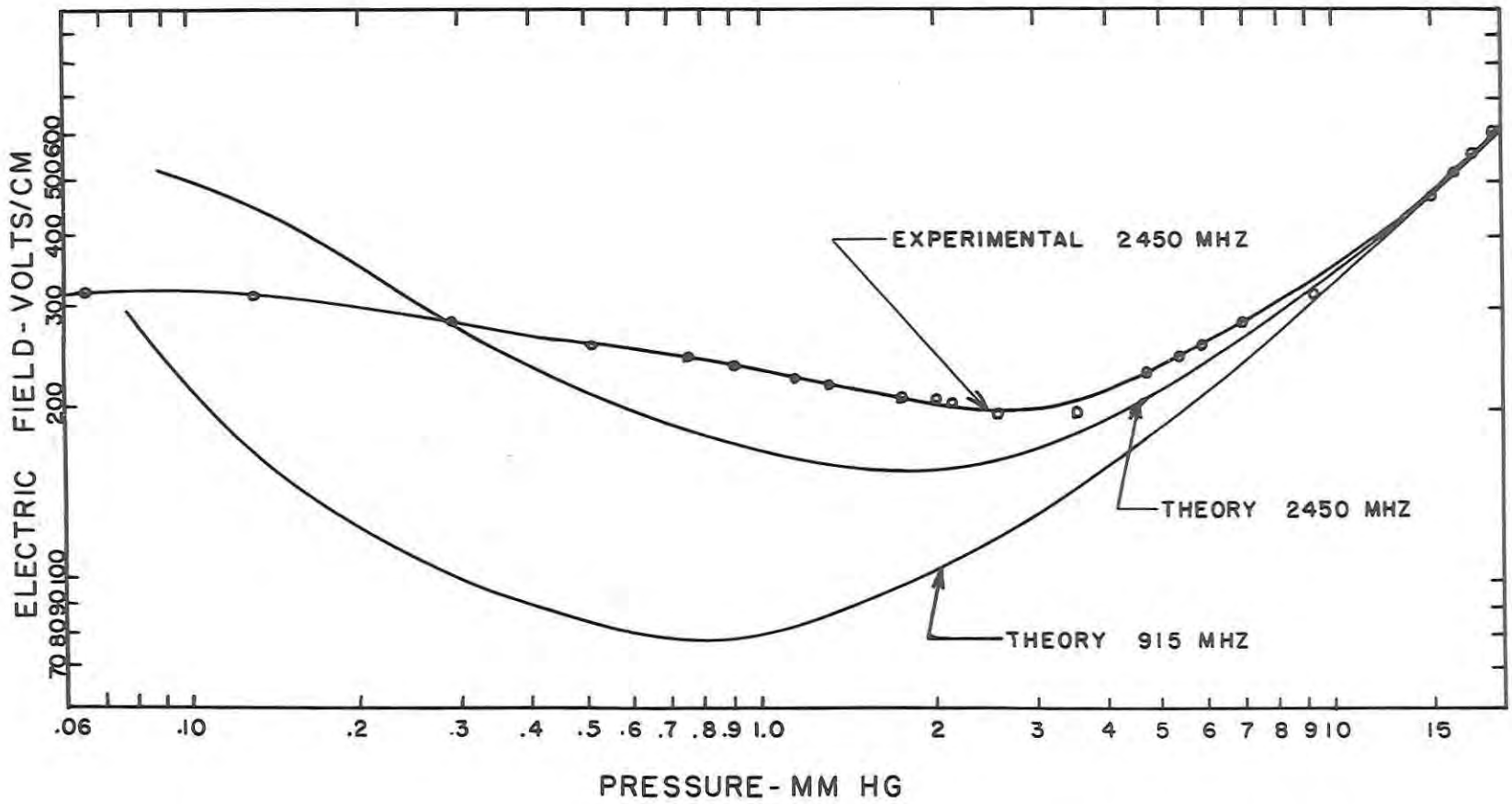

Figure 2. Experimental and theoretical breakdown fields for air at 915 MHz and 2450 MHz

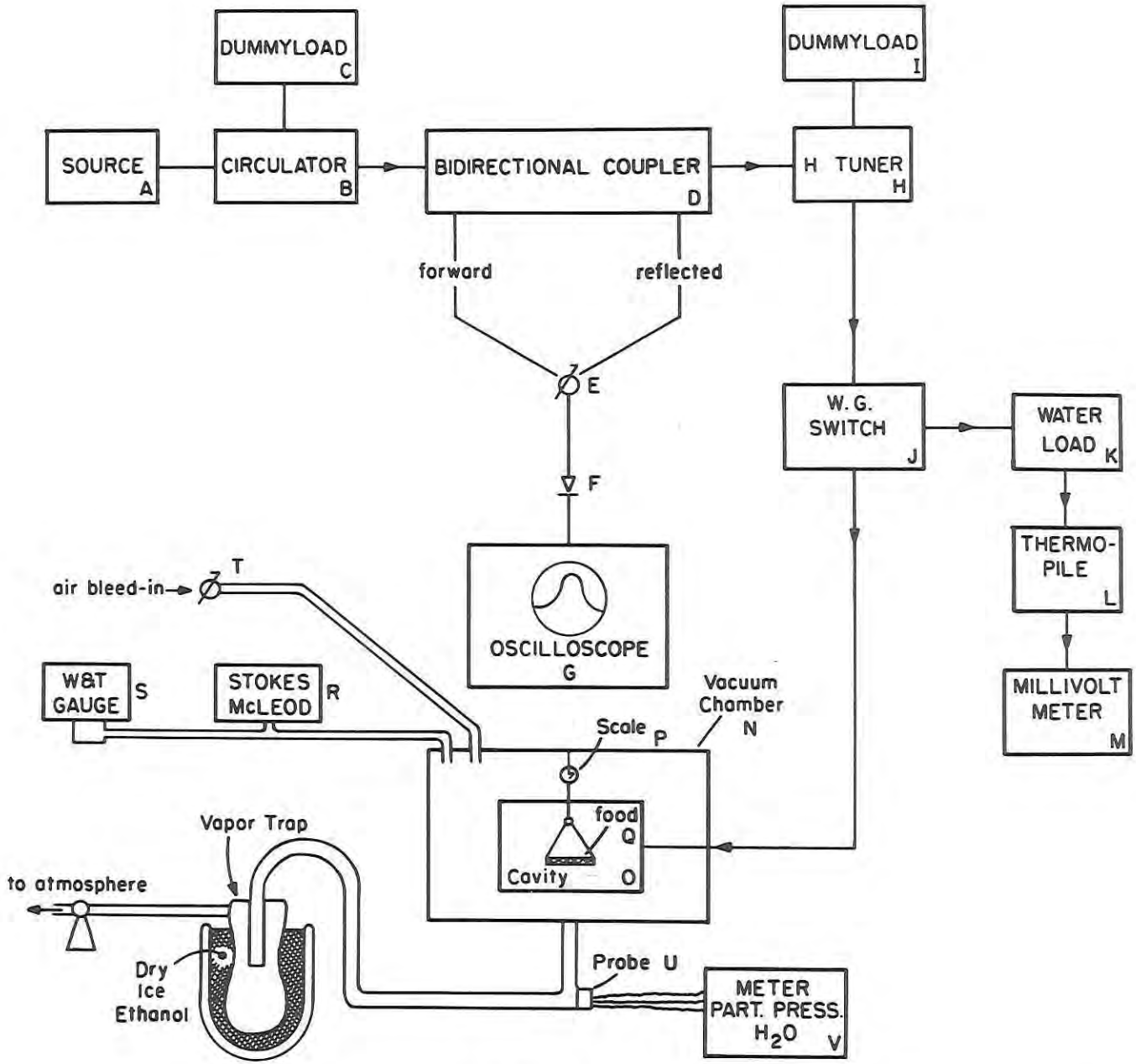

Figure 3. Block diagram of experimental microwave freeze drier

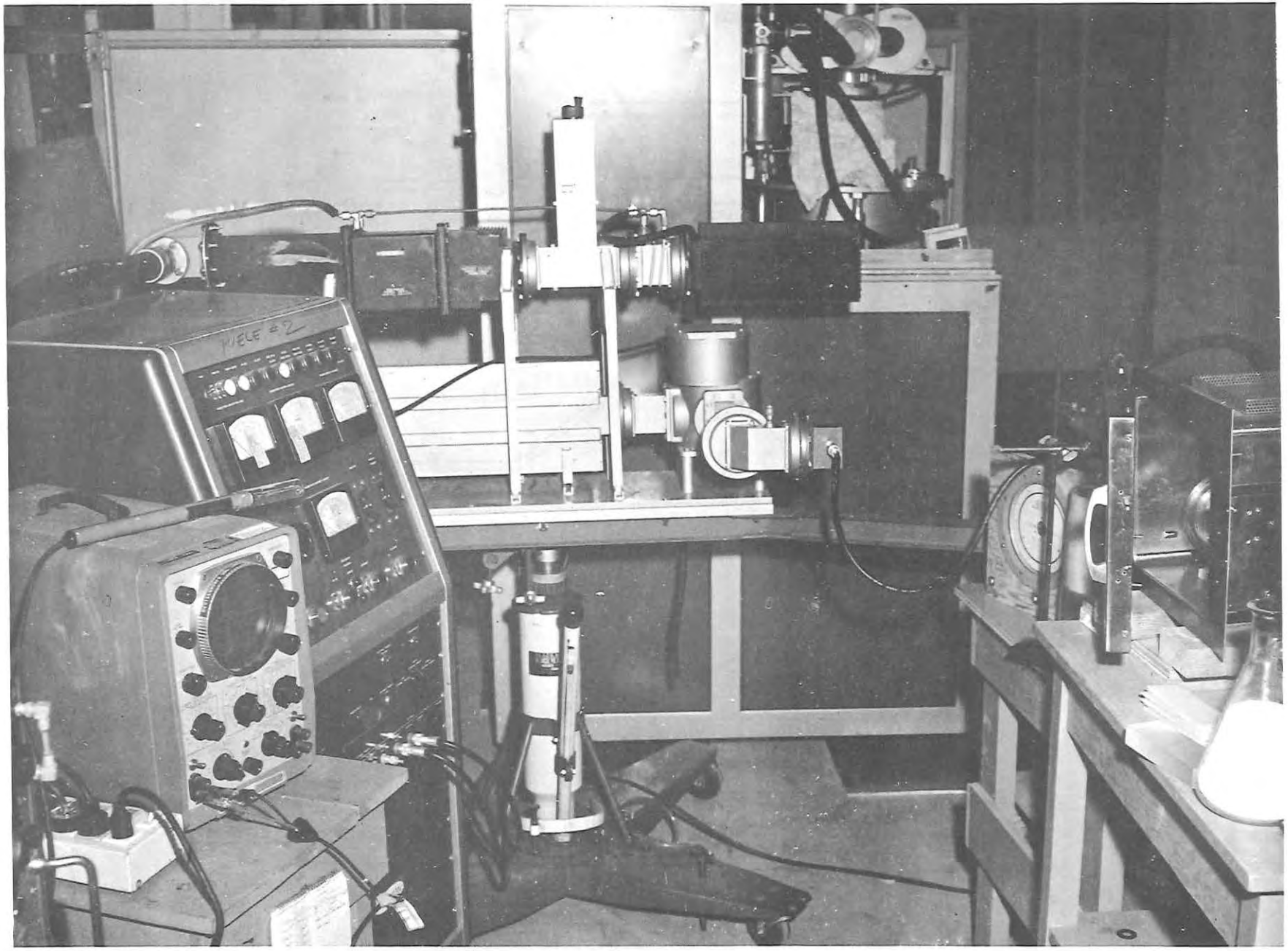

Figure 4. View of control console, bidirectional coupler, dummy loads, waveguide switch and water load

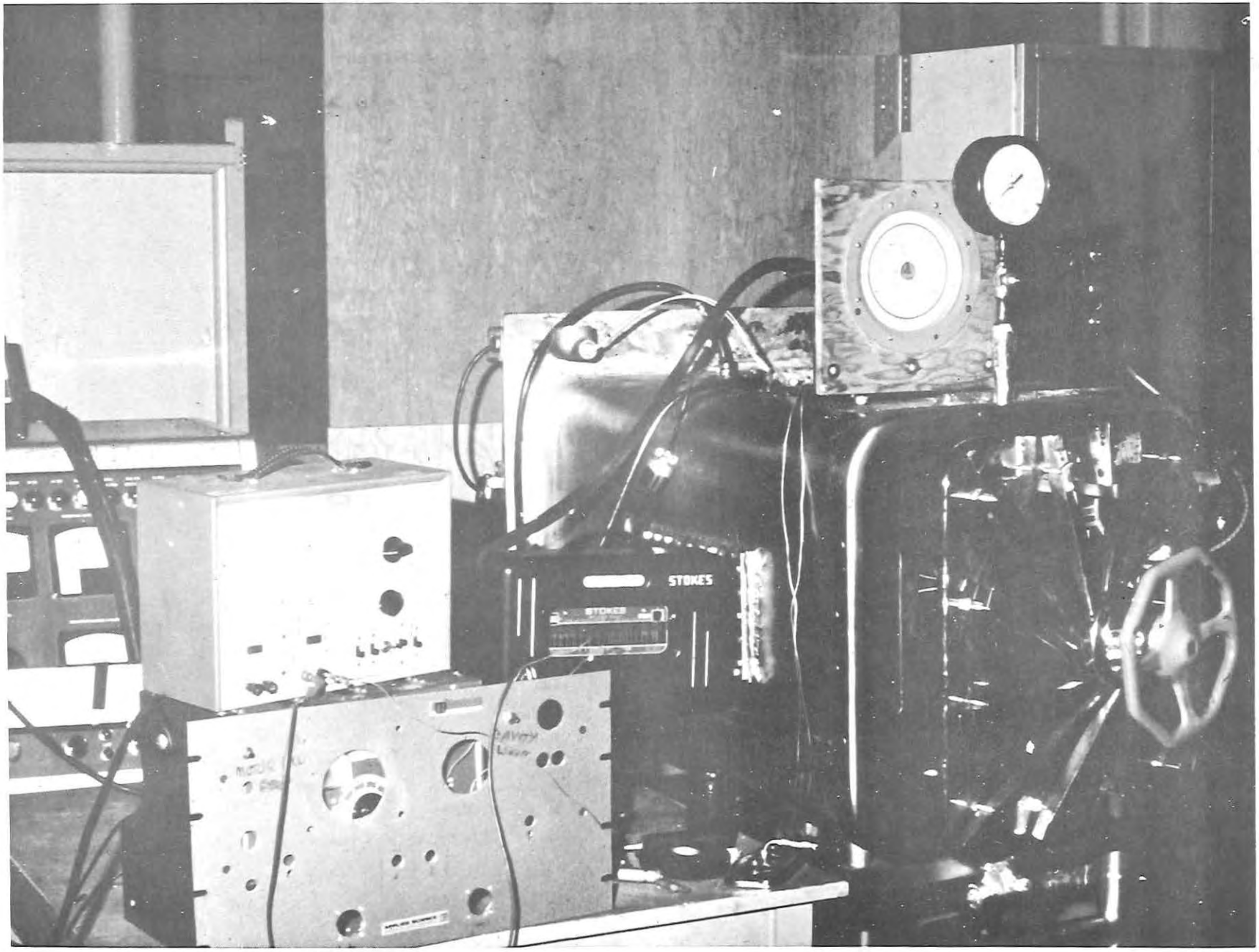

Figure 5. View of vacuum chamber and condenser

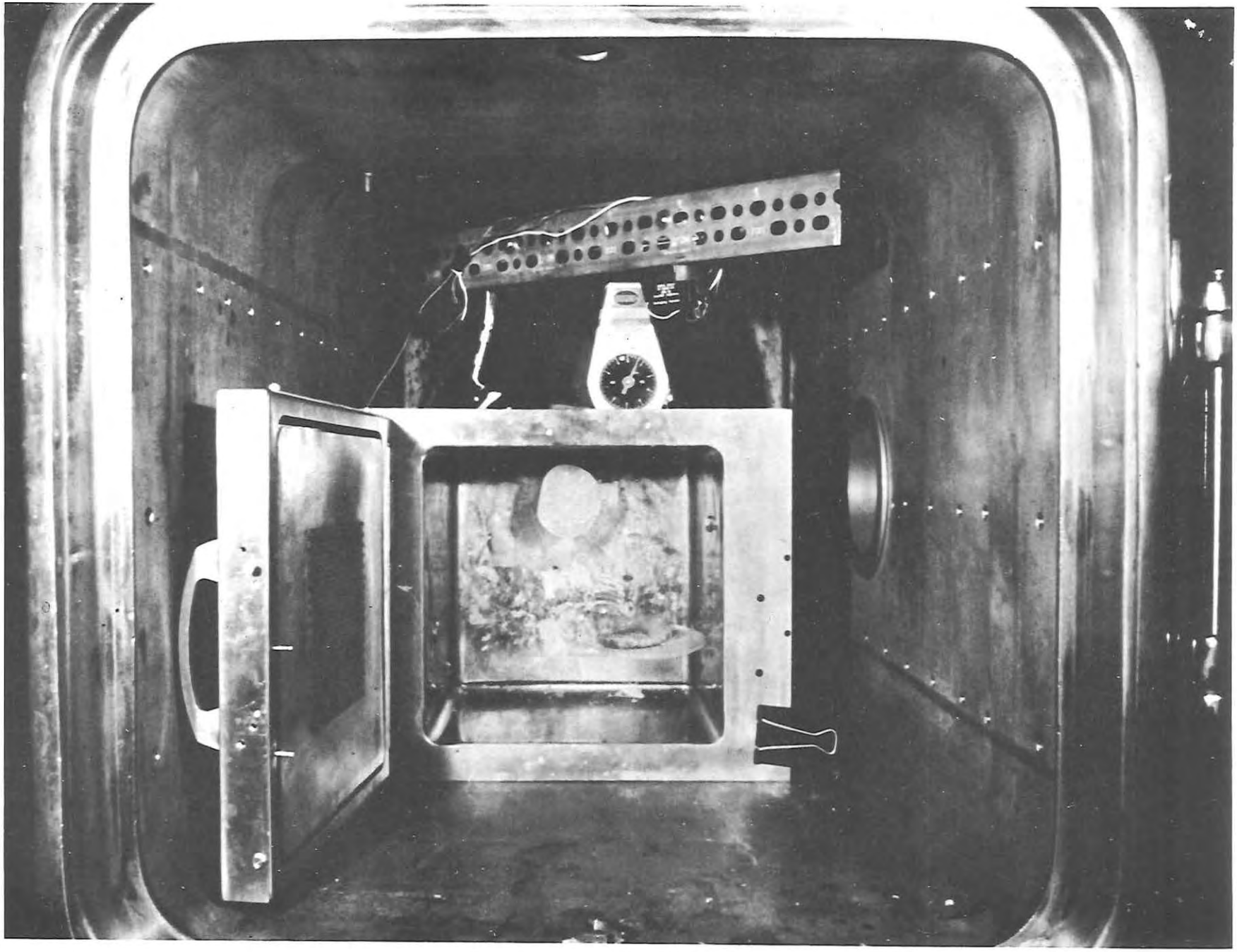

Figure 6. Front view of cavity showing food tray, scale, and rotator

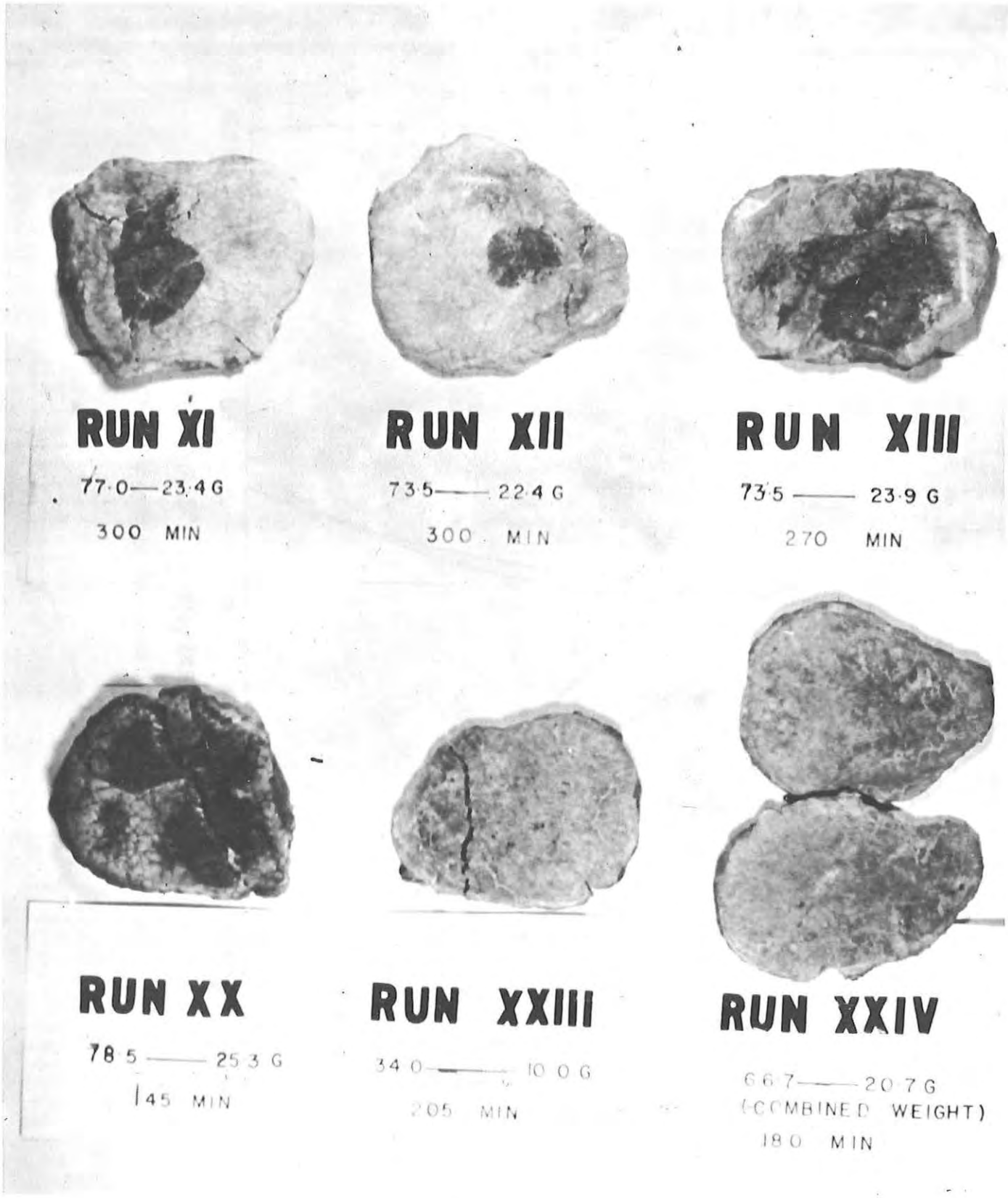

Figure 7. Freeze dried steaks from determination of maximum drying rate; runs XI, XII, XIII and XX violated triple point; runs XXIII and XXIV did not

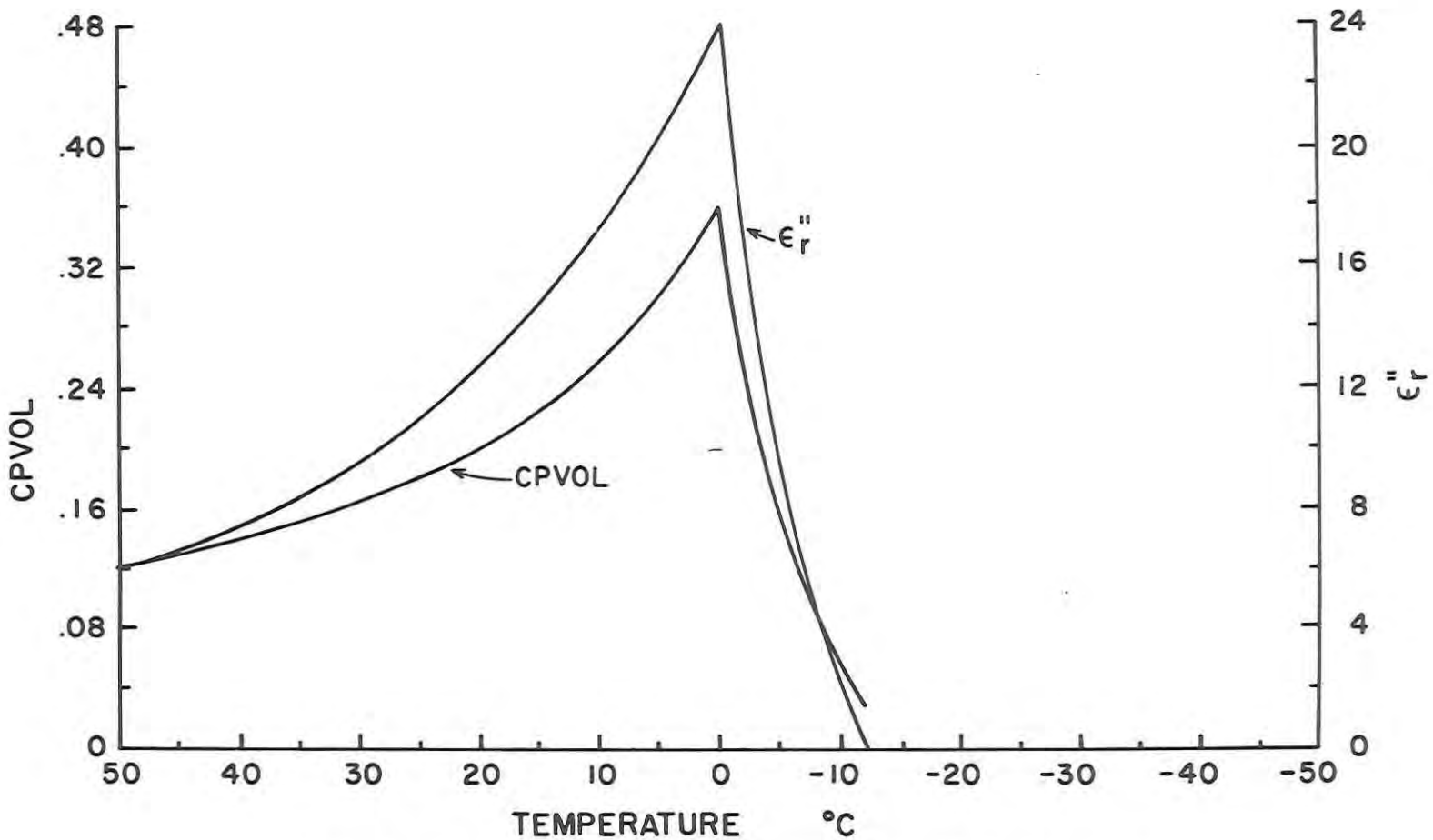

Figure 8. $\beta\epsilon''_c$ and loss factor, ϵ''_r, vs temperature for raw steak

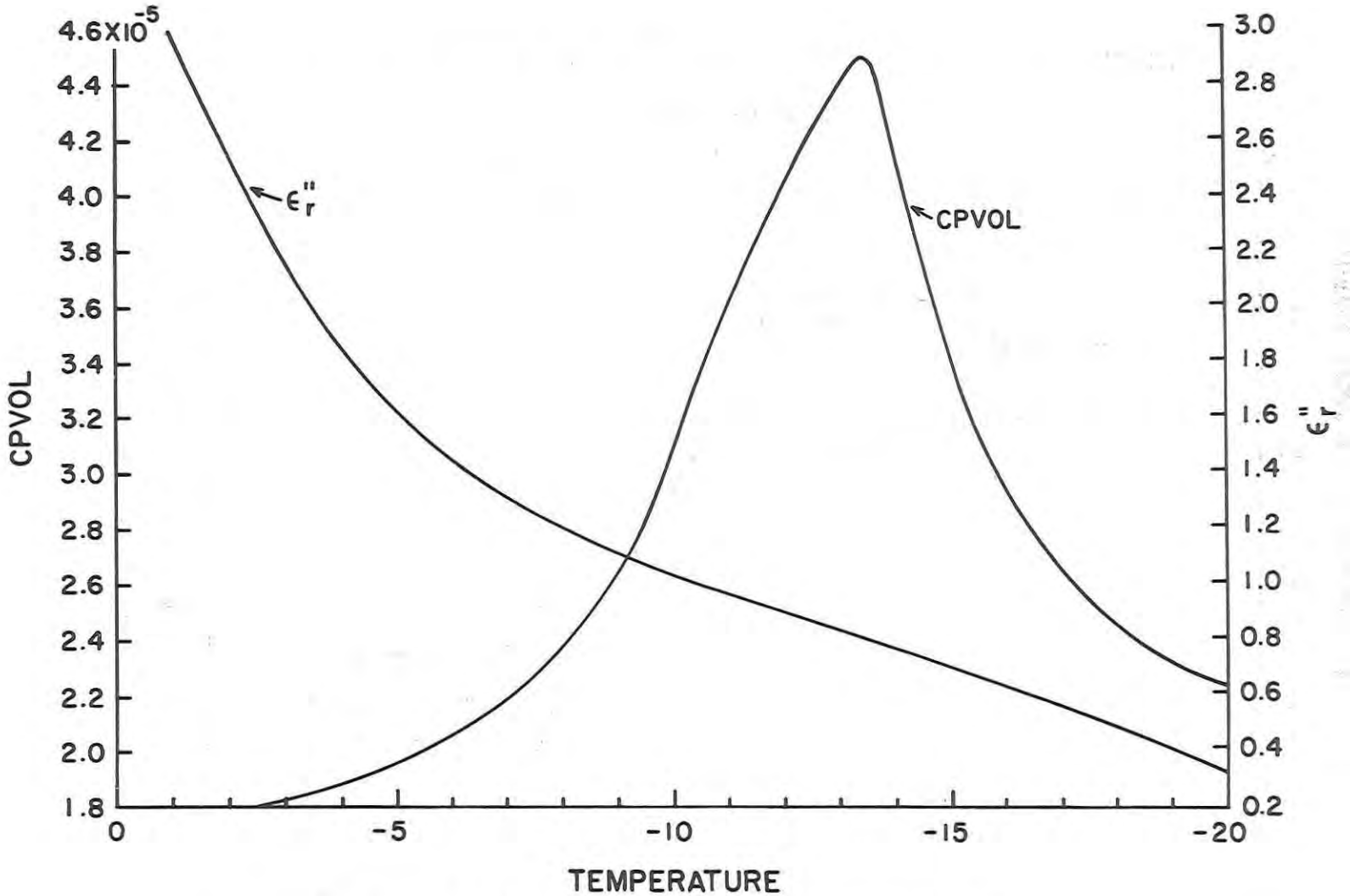

Figure 9. $\beta\epsilon_c''$ and loss factor, ϵ_r'', va temperature for H_{20}

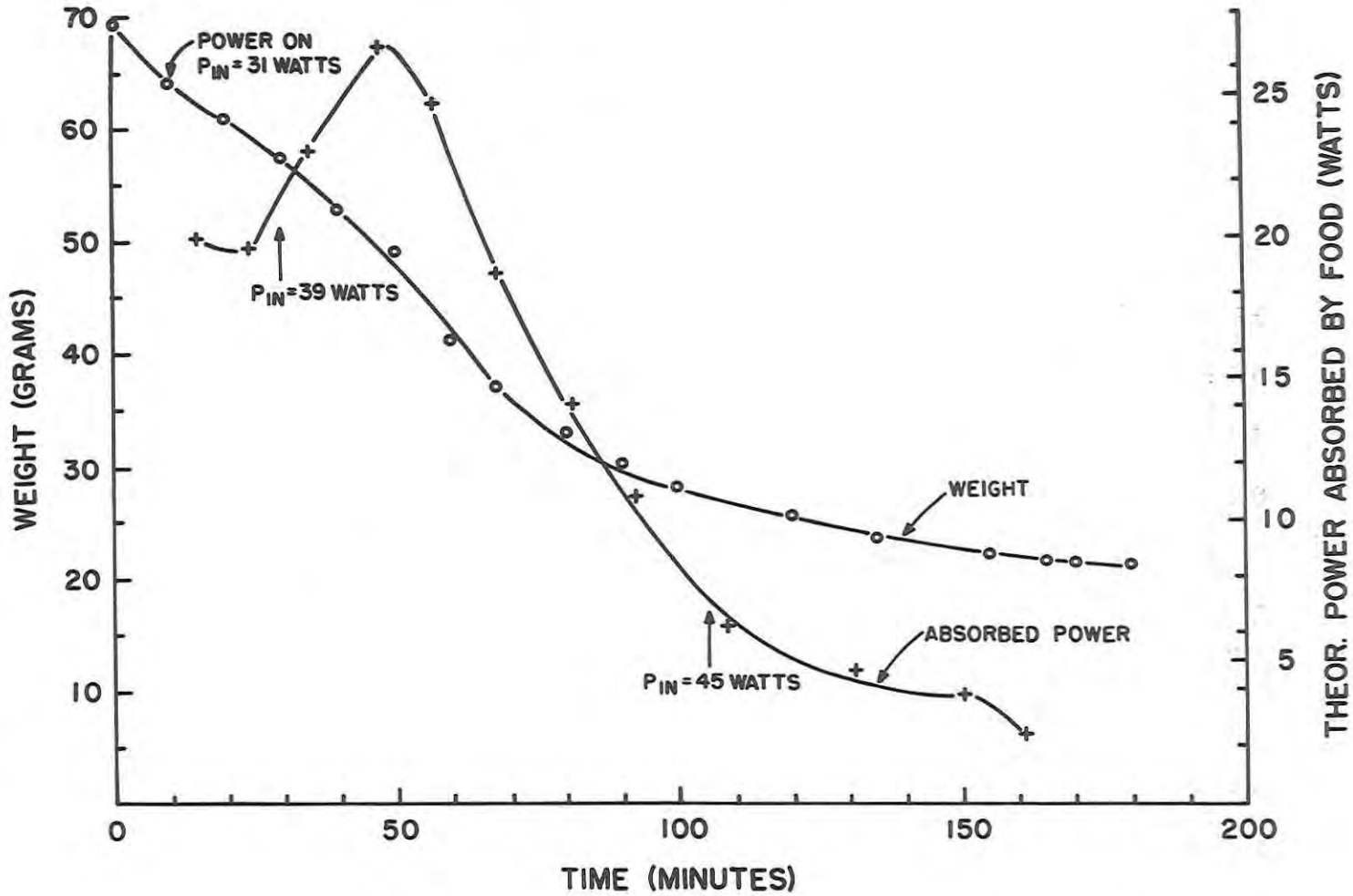

Figure 10. Weight of food and power absorbed by the food vs time for a typical freeze dry cycle with two 1/4-inch steaks

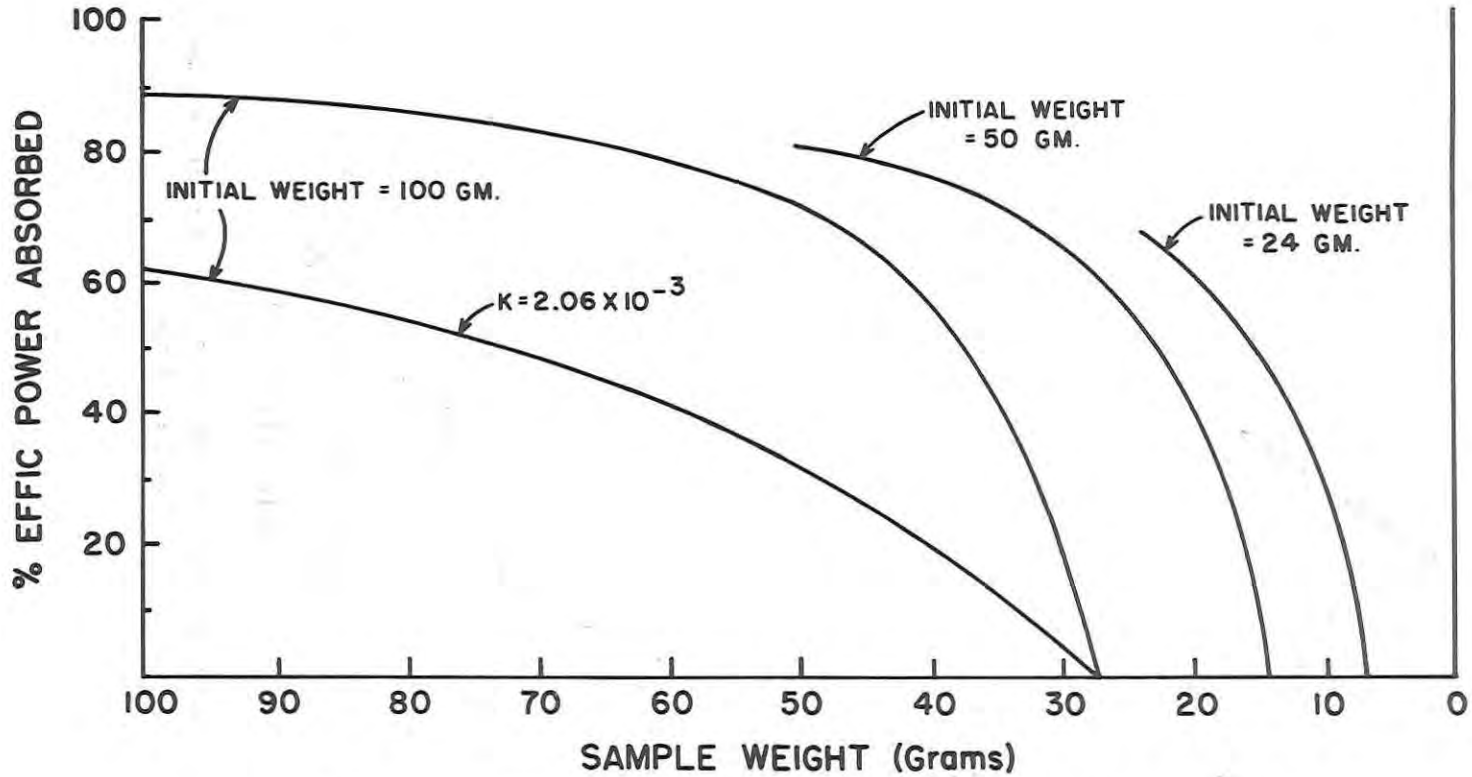

Figure 11. Efficiency of power absorption vs weight. $K = 0.39 \times 10^{-3}$

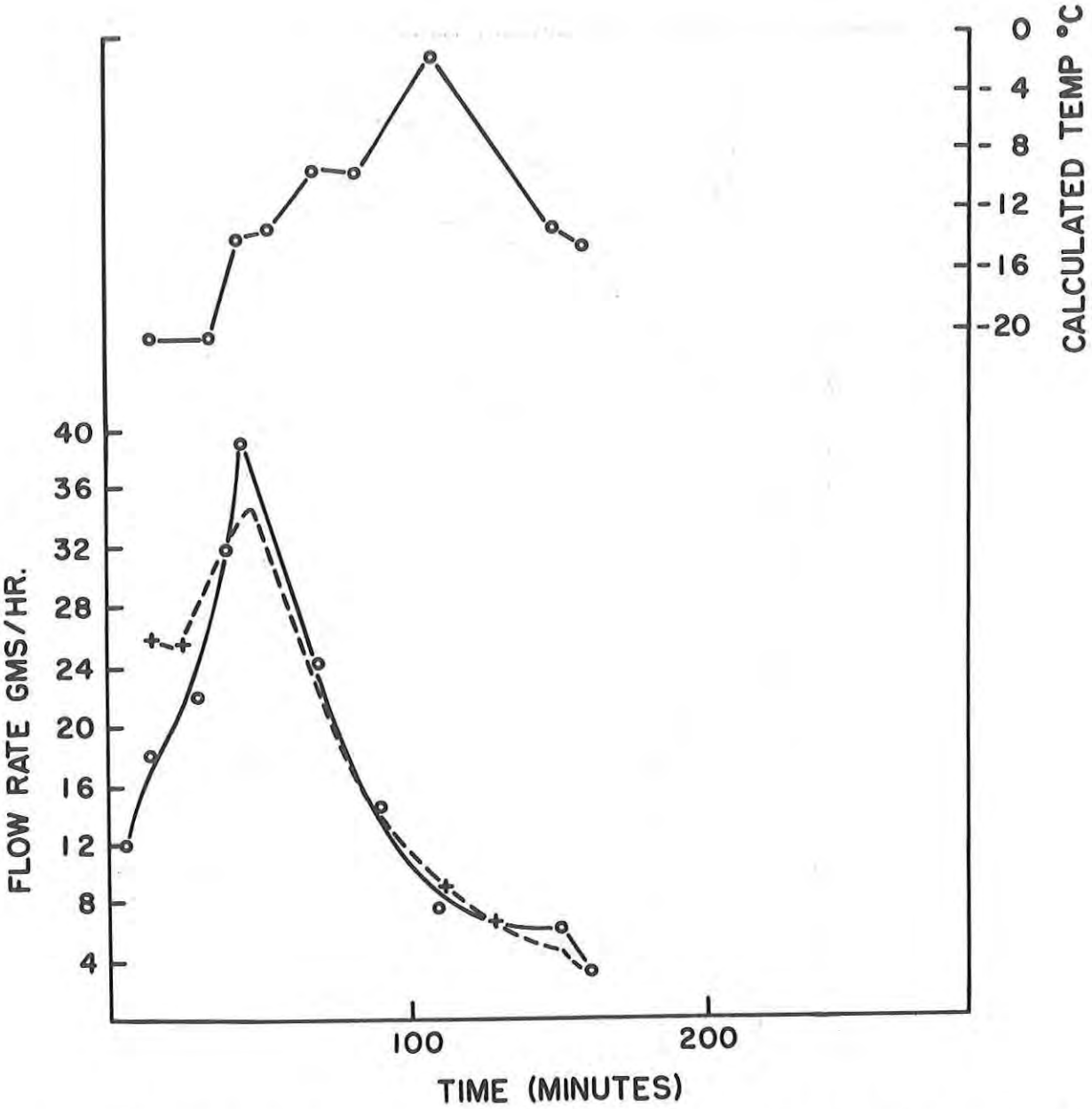

Figure 12. Measured flow rate, M_a and theoretical flow rate, M_e vs time for a typical freeze drying cycle of two 1/4-inch thick steaks

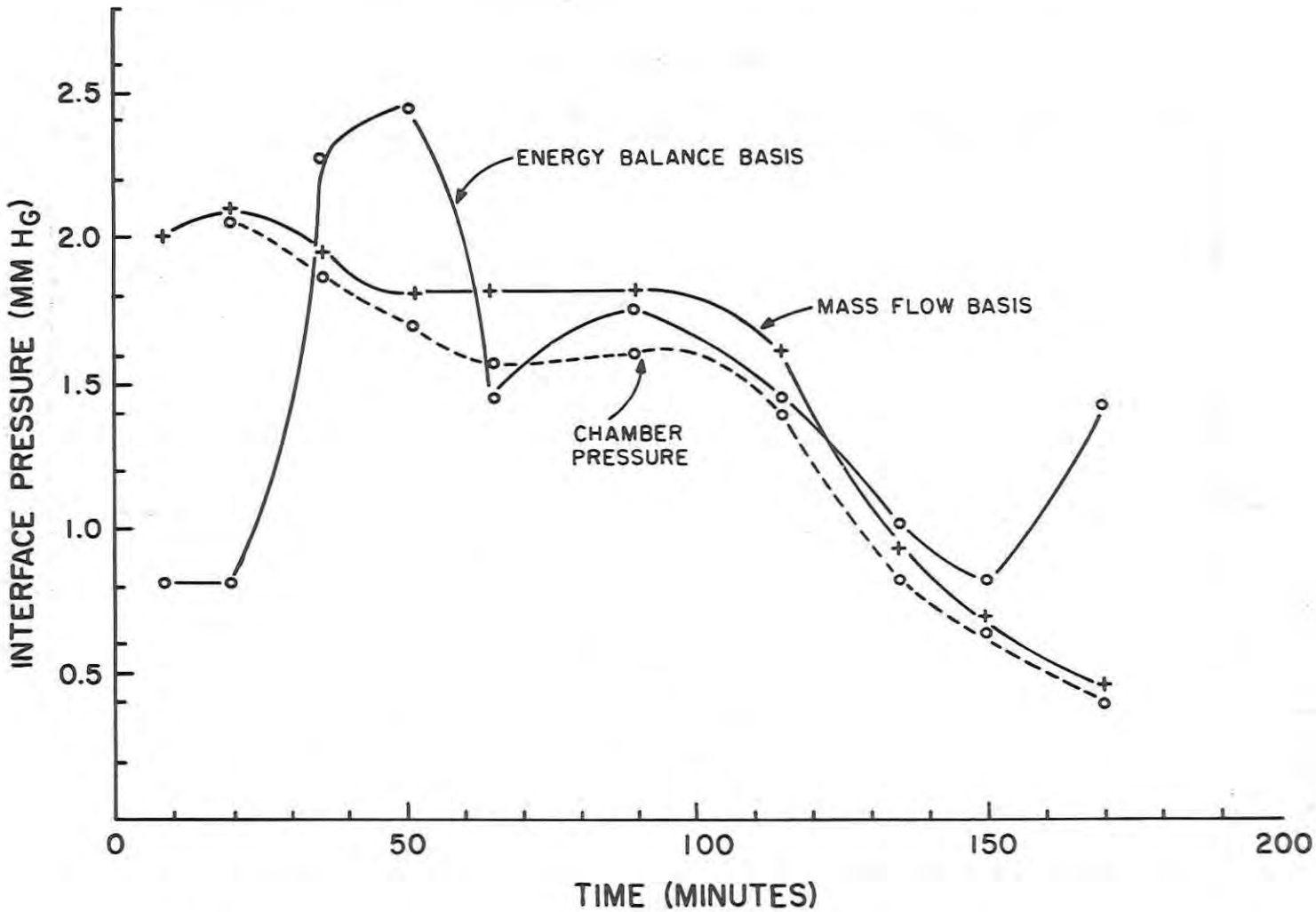

Figure 13. Interface pressures calculated on energy balance basis and a mass flow rate basis vs time for a typical freeze drying cycle. Measured chamber pressure is also shown.

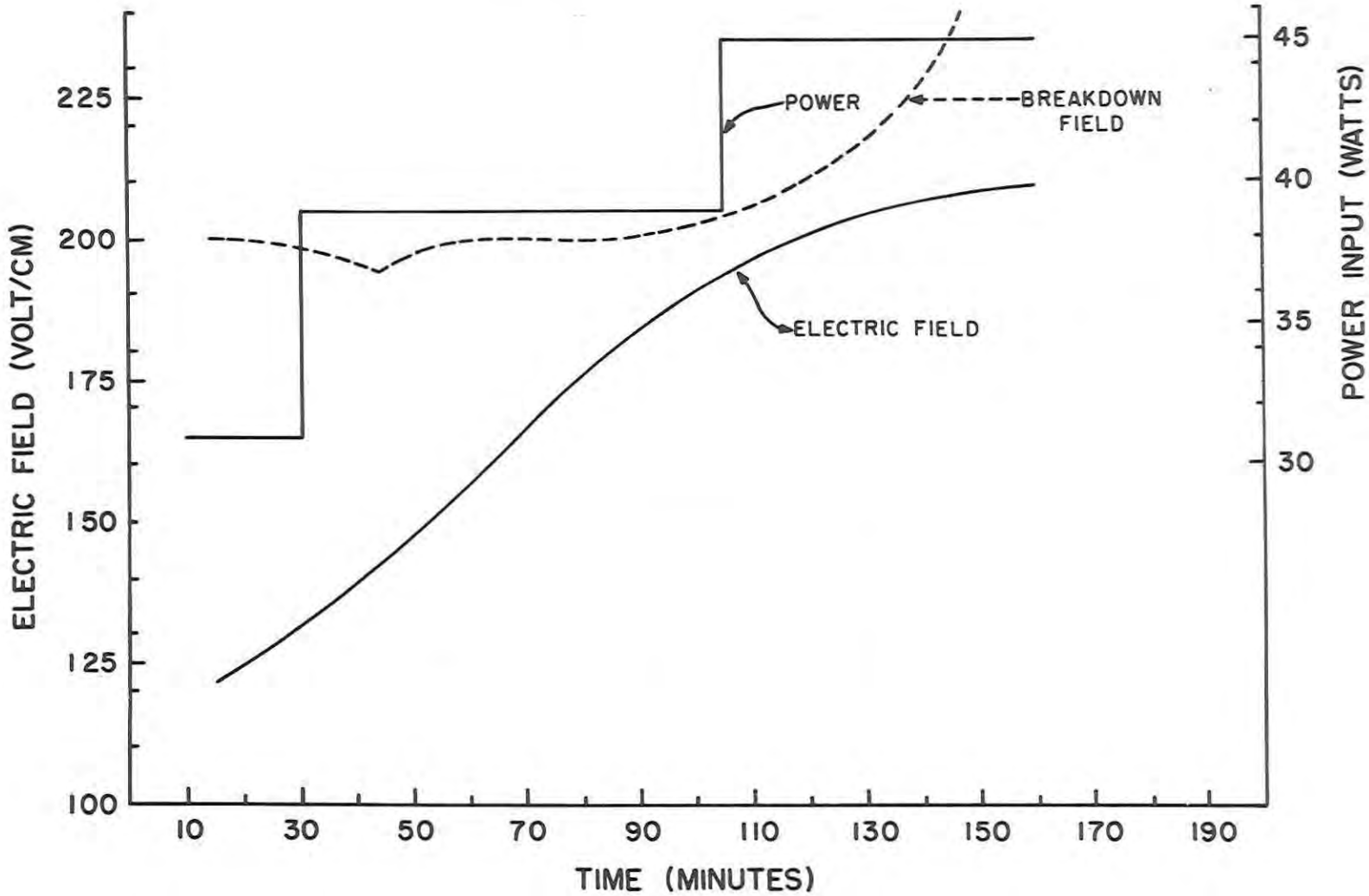

Figure 14. Electric field, breakdown field, and power input vs time for a typical freeze drying cycle for two 1/4-inch thick steaks.

FOOD LABORATORY DISTRIBUTION LIST

PROCESS DEVELOPMENT

Copies

1 - Commanding General
US Army Medical Research and Development Command
ATTN: MEDDH–SI
Washington, D.C. 20315

2 - Commanding General
US Army Test and Evaluation Command
ATTN: AMSTE-BC
Aberdeen Proving Ground, Maryland 21005

1 - Commanding General
US Army Combat Development Command
Combat Service Support Group
Fort Lee, Virginia 23801

1 - Commanding General
US Army Combat Development Command
ATTN: CDCMR-O
Fort Belvoir, Virginia 22060

1 - Commanding General
US Army Materiel Command
ATTN: AMCRD-JI
Department of the Army
Washington, D.C. 20315

2 - Commanding Officer
Edgewood Arsenal
ATTN: SMUEA-TSTI–TL
Aberdeen Proving Ground, Maryland 21010

Copies

1 - Commanding Officer
US Army Combat Development Command
Supply Agency
ATTN: CDCSA-R
Fort Lee, Virginia 23801

1 - Commanding Officer
US Army Medical Nutrition Laboratory
Fitzsimons General Hospital
Denver, Colorado 80240

1 - Commander
Defense Personnel Support Center
ATTN: Directorate of Subsistence, DPSC-STS
2800 South 20th Street
Philadelphia, Pennsylvania 19101

1 - Commandant of the Marine Corps
Headquarters US Marine Corps
ATTN: Code A04G
Washington, D.C. 20380

1 - Commandant of the Marine Corps
Headquarters US Marine Corps
ATTN: Code AX-4E5
Washington, D.C. 20380

1 - Deputy Chief of Staff, R&D
Headquarters, USAF (AFRDDG)
Washington, D.C. 20330

Copies

1 - Chief, Biomedical Sciences Division
Office of Assistant Director (Chemical Technology)
Room 3D-129, The Pentagon
Washington, D.C. 20301

2 - Executive Secretary
Interdepartmental Committee on Radiation Preservation of Food
Consumer Products Division 623
Business and Defense Service Administration
US Department of Commerce
Washington, D.C. 20230

2 - Subsistence Management Policy Director
ATTN: OASD (I&L)
Pentagon 2B323
Washington, D.C. 20301

1 - Director, AF Hospital Food Service
ATTN: Lt. Col. Chaska
Headquarter USAF/SGB-1
6B153 James Forrestal Building
Washington, D.C. 20314

2 - Director
Development Center
Marine Corps Development and Education Command
Quantico, Virginia 22134

1 - Director
Division of Biology and Medicine
US Atomic Energy Commission
Washington, D.C. 20545

Copies

1 - Director
US Army Advanced Materiel Concepts Agency
Washington, D.C. 20315

1 - Air Force Services Office
ATTN: Food Branch
2800 South 20th Street
Philadelphia, Pennsylvania 19101

2 - GET Division
Foreign Science and Technology Center
ATTN: AMXST-GE (Victoria Winters)
Building T-7
Washington, D.C. 20315

1 - Chief, Life Sciences Division
Army Research Office
Office of Chief of Research and Development
Washington, D.C. 20310

1 - Chief, Food Service Division
Walter Reed General Hospital
Washington, D.C. 20012

1 - Stimson Library
ATTN: Documents Librarian
US Army Medical Field Service School
Brooke Army Medical Center
Fort Sam Houston, Texas 78234

2 - Quartermaster School Library
US Army Quartermaster School
Fort Lee, Virginia 23801

2 - Technical Library
USACDC Institute of Land Combat
301 Taylor Drive
Alexandria, Virginia 22314

Copies

1 - US Naval Research Laboratory
Code 6140
Washington, D.C. 20390

1 - US Department of Agriculture
Division of Acquisitions
National Agriculture Library
Washington, D.C. 20250

3 - Office of the Coordinator of Research
University of Rhode Island
Kingston, Rhode Island 02881

1 - Library Southern Utilization Research and Development Division
Agricultural Research Service
US Department of Agriculture
P.O. Box 19687
New Orleans, Louisiana 70119

2 - Department of the Army
Headquarters, Fort Detrick
ATTN: Documents, Technical Library
Frederick, Maryland 21701

2 - US Army Research Office
ATTN: Technical Library
3045 Columbia Pike
Arlington, Virginia 22204

1 - The Surgeon General
Department of the Army
ATTN: DASG-HEP-H
Washington, D.C. 20314

1 - Headquarters, Air Force Systems Command
ATTN: Col. Robert McIver
Andrews Air Force Base, Maryland 20331

Copies

1 - Headquarter, AMD-RD
Brooks Air Force Base, Texas 78235

1 - Headquarters Defense Supply Agency
ATTN: Mr. Jobe, DSAH-OP
Cameron Station
Alexandria, Virginia 22314

2 - Headquarters 12th Support Brigade
ACofS Service
ATTN: Food Advisor
Fort Bragg, North Carolina 28307

4 - Exchange and Gift Division
Library of Congress
Washington, D.C. 20540

1 - R. J. Reynolds Tobacco Company
ATTN: J. E. Roberts
Winston-Salem, North Carolina 27101

1 - Colonel William S. Augerson, MC, USA
Military Assistant for Medical and Life Sciences
OAD/E&IS, The Pentagon (Rm 3B129)
Department of Defense Research and Engineering
Washington, D.C. 20301

1 - CDR Harold J. Janson, MSC, USN
Head, Food Service Branch
Bureau of Medicine & Surgery
Navy Department
Washington, D.C. 20390

Copies

1 - Commandant of the Marine Corps
Headquarters U.S. Marine Corps
ATTN: Code COB-2
Washington, D.C. 20380

1 - Commandant of the Marine Corps
Headquarters U.S. Marine Corps
ATTN: CSY-4
Washington, D.C. 20380

1 - Commanding General
Marine Corps Supply Activity
ATTN: Code 826
1100 South Broad Street
Philadelphia, Pennsylvania 19146

FOOD LABORATORY INTERNAL DISTRIBUTION LIST

PROCESS DEVELOPMENT

22- Program Coordination Office, Food Laboratory, NLABS (12 for transmittal to Defense Documentation Center)

2 - Technical Library, NLABS

7 - Division Chiefs, Food Laboratory, NLABS

2 - Marine Liaison Officer, NLABS

3 - Air Force Liaison Officer, NLABS

1 - Special Assistant for DOD Food Program, ATTN: Dr. E. E. Anderson, NLABS

1 - US Army Representative for DOD Food Program, ATTN. Col. M. B. Michl, NLABS

1 - US Air Force Representative for DOD Food Program, ATTN: LTC R. E. Pop, NLABS

1 - US Navy Representative for DOD Food Program, ATTN: LCDR K. West, NLABS

2 - Chief, Quality Assurance and Engineering Office, ATTN: Standardization Management and Quality Assurance Branch (Mr. Richman), NLABS

3 - Director, General Equipment and Packaging Laboratory, NLABS

3 - Director, Pioneering Research Laboratory, NLABS

25- Project Officer, Food Laboratory, NLABS

10- Alternate Project Officer, Food Laboratory, NLABS

Security Classification

DOCUMENT CONTROL DATA - R & D

(Security classification of title, body of abstract and indexing annotation must be entered when the overall report is classified)

1. ORIGINATING ACTIVITY *(Corporate author)* U.S. Army Natick Laboratories Natick, MA 01760	2a. REPORT SECURITY CLASSIFICATION Unclassified 2b. GROUP

3. REPORT TITLE

MICROWAVE FREEZE DEHYDRATION AT 2450 MHZ

4. DESCRIPTIVE NOTES *(Type of report and inclusive dates)*

5. AUTHOR(S) *(First name, middle initial, last name)*

James W. Gould, John T. Perry, Jr. and Ernest M. Kenyon

6. REPORT DATE November 1971	7a. TOTAL NO. OF PAGES	7b. NO. OF REFS
8a. CONTRACT OR GRANT NO. b. PROJECT NO. 1J662713A034 Code: 2072450271 c. d.	9a. ORIGINATOR'S REPORT NUMBER(S) 9b. OTHER REPORT NO(S) *(Any other numbers that may be assigned this report)*	

10. DISTRIBUTION STATEMENT

This document has been approved for public release and sale; its distribution is unlimited.

11. SUPPLEMENTARY NOTES	12. SPONSORING MILITARY ACTIVITY

13. ABSTRACT

A generalized model of microwave freeze dehydration is presented including the efficiency of power absorption, the mass flow rates of water and water vapor, and the parameters characterizing corona breakdown at the 2450 MHz operating frequency. The effect of chamber pressure, gas composition, size and thickness of the food load, and the operating frequency are discussed theoretically and compared to experimental data for freeze dehydration at 2450 MHz. The agreement between the theoretical and experimental mass flow rates was good for the majority of the dehydration cycle.

DD FORM 1 NOV 65 1473 REPLACES DD FORM 1473, 1 JAN 64, WHICH IS OBSOLETE FOR ARMY USE.

Security Classification